

Antiferromagnetic integer-spin chains in a staggered magnetic field: approaching the thermodynamic limit through the infinite-size DMRG.

Massimo Capone and Sergio Caprara

Dipartimento di Fisica, Università di Roma “La Sapienza”, and Istituto Nazionale per la Fisica della Materia (INFM), Unità di Roma 1, Piazzale Aldo Moro 2, I-00185 Roma, Italy

(November 13, 2018)

We investigate the behavior of antiferromagnetic integer-spin chains in a staggered magnetic field, by means of the density-matrix renormalization group, carefully addressing the role of finite-size effects within the Haldane phase at small fields. In the case of spin $S = 2$, we determine the dependence of the groundstate energy and magnetization on the external field, in the thermodynamic limit, and show how the peculiar finite-size behavior can be connected with the crossover in the groundstate from a spin liquid to a polarized Néel state.

75.10.Jm, 75.30.Cr, 75.40.Mg

I. INTRODUCTION

The behavior of antiferromagnetic (AFM) Heisenberg spin chains is dominated by quantum fluctuations which suppress magnetic long-range order. However, after Haldane’s proposal [1], it has become clear that the value of the spin S plays a crucial role. Integer and half-integer spin cases are indeed completely different. The spectrum of the half-integer spin chain is gapless in the thermodynamic limit, and the system is critical, in the sense that the linear response to an infinitesimal staggered magnetic field, coupled to the would-be order parameter, is divergent (at zero temperature). Conversely, the integer-spin chain has a spectrum which stays gapped in the thermodynamic limit. The first excited state has a finite distance from the groundstate (the so-called Haldane gap), and the system is not critical, i.e., the linear response to an infinitesimal staggered magnetic field is finite. The groundstate, which is characterized by a finite correlation length, is a spin liquid.

The two behaviors are only reconciled as $S \rightarrow \infty$. This limiting case, which corresponds to the suppression of quantum fluctuations, leads to the closure of the Haldane gap and to the divergence of the staggered susceptibility even in the integer-spin case, which becomes thus indistinguishable from the half-integer-spin case, as it is naively expected at large S .

All theoretical approaches are well controlled only in the limit of large S , while the increasing relevance of quantum fluctuations makes the predictions less accurate as S is reduced. On the other hand, the introduction of the staggered magnetic field gradually freezes quantum fluctuations, and the problem arises of the description of the spin-liquid state in a staggered magnetic field and its evolution to the frozen state. A non-linear σ -model approach has been recently developed to investigate this evolution [2]. This approach relies on the Haldane *ansatz*, and becomes exact in the limit $S \rightarrow \infty$, in the absence of staggered magnetic field. However, the validity of the *ansatz* must be limited by some finite field, at which the

spin-liquid description breaks down. Moreover, at small S , the starting *ansatz* is (quantitatively) not appropriate even at zero field, and corrections must be considered, when describing the field-driven crossover from the spin liquid to the polarized AFM state.

This paper is therefore devoted to the numerical analysis of the response of the AFM integer-spin chains to a staggered magnetic field, by means of the density-matrix renormalization group (DMRG) [3], which gives basically exact results for one-dimensional systems, that are not biased by any *a priori* assumption, and represent an almost ideal numerical test for analytical results.

The case $S = 1$ has been most extensively studied within DMRG [4], but the case $S = 2$ [5] represents quite a hard numerical task even in the absence of a magnetic field, and lacks any analysis in the presence of the staggered field, that will be the main object of our numerical investigation.

Our starting Hamiltonian reads

$$\mathcal{H} = J \sum_{i=1}^{L-1} \mathbf{S}_i \cdot \mathbf{S}_{i+1} - H \sum_{i=1}^L (-1)^i S_i^z, \quad (1)$$

where \mathbf{S}_i is the spin- S operator on site i , $S = 1, 2, \dots$ is integer, and L is the number of sites in the chain. $J > 0$ is the AFM Heisenberg coupling, H is the amplitude of the staggered magnetic field along the z axis, which is coupled with the staggered magnetization $M^z = \sum_i (-1)^i S_i^z$. In view of the forthcoming DMRG study, we explicitly assumed open boundary conditions (OBC) in writing the first term in (1).

The Hamiltonian (1) is manifestly not invariant under reflection with respect to the mid point of the chain when L is even. However, in the standard implementation of the DMRG algorithm [3], L is even, and the reflection symmetry is used to reduce the numerical effort by identifying the right block with the reflection of the left one (for more details, see the discussion in Sec. II). Although there is no problem in implementing a non-symmetric algorithm [6,7], the Hamiltonian (1) can be easily made invariant under reflection by means of

a simple gauge transformation (i.e. a local rotation of the reference frame), given by $(-1)^i S_i^z \rightarrow \tilde{S}_i^z$, and, e.g., $(-1)^i S_i^x \rightarrow \tilde{S}_i^x$, while \tilde{S}_i^y coincides with S_i^y . Once the transformation is performed, the Hamiltonian (1) is recast in the form

$$\tilde{\mathcal{H}} = -J \sum_{i=1}^{L-1} \left[\tilde{S}_i^z \tilde{S}_{i+1}^z + \frac{1}{2} \left(\tilde{S}_i^+ \tilde{S}_{i+1}^+ + \tilde{S}_i^- \tilde{S}_{i+1}^- \right) \right] - H \sum_{i=1}^L \tilde{S}_i^z, \quad (2)$$

where $\tilde{S}_i^\pm = \tilde{S}_i^x \pm i\tilde{S}_i^y$, and the external field is now coupled to the uniform magnetization $\tilde{S}^z = \sum_i \tilde{S}_i^z$. The token we pay to recover reflection symmetry is the appearance of terms of the form $S_i^+ S_{i+1}^+$ and $S_i^- S_{i+1}^-$, in which the spin is simultaneously raised or lowered on neighboring sites.

The original Hamiltonian (1) commutes with the z -component of the total spin $S^z = \sum_i S_i^z$ and, therefore, the gauge-transformed Hamiltonian (2) commutes with the staggered magnetization $\tilde{M}^z = \sum_i (-1)^i \tilde{S}_i^z$. It is easily realized that the groundstate of the model lies within the $\tilde{M}^z = 0$ subspace at large values of the field H . At zero field, the groundstate is instead degenerate (in the presence of OBC), but, since the total spin is obviously integer, a state with $\tilde{M}^z = 0$ is certainly present in the groundstate multiplet. We explicitly checked that (at least a component of) the groundstate always lies in the $\tilde{M}^z = 0$ subsector for every value of the amplitude of the external field H . Henceforth, for the sake of definiteness, we assume $H > 0$, the case of negative H being trivially recovered by changing $\tilde{S}^z \rightarrow -\tilde{S}^z$ and $\tilde{M}^z \rightarrow -\tilde{M}^z$ in the following discussion. In particular the groundstate energy and magnetization are even and odd functions of the external field respectively. In the rest of the paper we refer to the properties of the model described by (2), and in particular to the uniform magnetization along the external field, $\langle \tilde{S}^z \rangle$. The correspondence with the original model (1) is straightforward.

The plan of the paper is the following: in Sec. II we discuss the general problem of extracting the thermodynamic properties within the DMRG approach, in connection with the interplay of finite-size effects and truncation of the Hilbert space, and we specialize the discussion to the case of the Haldane spin-liquid phase at small magnetic field; in Sec. III we present our numerical results, mostly on the $S = 2$ case, and discuss the various regimes which characterize the model at small (Sec. III A) and large (Sec. III B) magnetic field, showing how these can be also characterized by the peculiar form of the finite-size corrections to the magnetization; concluding remarks are found in Sec. IV.

We point out that throughout the paper, whenever we discuss finite-size corrections, we specifically refer to corrections in the presence of OBC, which are those affecting our DMRG results.

II. EXTRACTING THE THERMODYNAMIC PROPERTIES

After the introduction, by S. R. White [3], of the DMRG, a wide majority of the DMRG studies focused on the so-called finite-size algorithm, in which the system size is first increased until a chosen size is reached, and then stopped. Subsequently, a few further ‘‘sweeps’’ are performed to improve the basis for that system size. On the other hand, in the infinite-size algorithm the size is always increased at each step. It is clear that, for a given lattice size, the finite-size algorithm gives the best estimate (at fixed Hilbert space). Conversely, if one is really interested in the thermodynamic limit, the information obtained with the infinite-size algorithm are of extreme value [8,9], and become crucial in the integer-spin case at issue in this paper, as we show below. We point out that extreme care has to be taken in checking the convergence of the procedure with respect to the truncation of the Hilbert space, before any sensible statement on the physical meaning of the numerical results is made.

The algorithm we used is the standard implementation of the infinite-size DMRG, which is described in [3] (see also [6,7]). Here we limit ourselves to a quick summary which serves as an introduction to the notations which we use in the paper. As it is customary we start with a 4-site chain which is divided into a left and a right part (blocks). The density matrix of, say, the right block in the groundstate of the entire system (superblock) is diagonalized and N_k eigenstates, corresponding to the largest eigenvalues, are kept as the most representative of the block, while the other eigenstates are truncated away, thus reducing the size of the Hilbert space. In the presence of reflection symmetry with respect to the mid point of the chain, the left block is simply the reflection of the right block. Once the truncated left and right blocks are obtained, two more sites are added in the middle of the chain, and the new left and right blocks are defined, each as the ‘‘old truncated block + newly added site’’ system. The procedure is then iterated. After N_{RG} iterations the chain contains $L = 2N_{RG} + 2$ sites. At each step, a measure of the reliability of the procedure is provided by the truncation error $\mathcal{R} = 1 - \sum_{i=1}^{N_k} w_i$, where w_i are the eigenvalues of the density matrix, sorted in decreasing order. It follows from the definition that $0 \leq \mathcal{R} \leq 1$, and that, in the most general case, $\mathcal{R} = 1$ only when all the basis states are kept at each iteration, unless, under special circumstances, a simplification occurs in the spectrum of the density matrix (see below, Sec. III B). The success of DMRG when dealing with one-dimensional systems is due to their peculiar topology in the presence of short-range interactions. In most cases, indeed, the truncation error can be made small by keeping a number of states N_k which is much smaller than the full size of the block Hilbert space $[(2S + 1)^{L/2}$ in the present case], and can

be considered, for all practical purposes, independent of the system size L at fixed \mathcal{R} . We point out, however, that a small value of \mathcal{R} does not by itself imply a good convergence with respect to the truncation of the Hilbert space, first of all because the convergence must be directly checked on the observed physical quantity, which may have a peculiar dependence on \mathcal{R} , and also because different observables have different rates of convergence [8].

The observables are extracted by means of the standard DMRG procedure [3]. In this paper we mainly discuss the groundstate energy

$$E_0(J, H; L, N_k) = \left\langle \left[\tilde{\mathcal{H}} \right]^T \right\rangle,$$

and magnetization

$$M(J, H; L, N_k) = \left\langle \left[\tilde{S}^z \right]^T \right\rangle,$$

where the symbol $\langle \cdot \rangle$ denotes the expectation value over the DMRG approximate groundstate wavefunction, for the system of size L , with N_k states retained in the density-matrix truncation procedure, and the superscript T means that the corresponding operator has been properly truncated onto the superblock basis.

In the following we define the groundstate energy per site in units of J , $e_0 = E_0/(JL)$, and the magnetization per site in units of S , $m = M/(SL)$, such that $0 \leq m \leq 1$. We also introduce the notation $h \equiv H/J$, since e_0 and m depend on J and H only through their ratio h .

A glance at the magnetization curves as a function of the system size L , for various magnetic fields, and a fixed number of states (e.g., $N_k = 50$, see Fig. 1), shows that there are two different behaviors at small and large field respectively. The convergence of the magnetization to the thermodynamic limit is non-monotonic at small h , and m is characterized by a well-pronounced bump at a characteristic length L_b which increases with increasing S and decreases with increasing h . This property strongly suggests that system sizes smaller than L_b are definitely not representative of the thermodynamic limit, and that only for $L \gg L_b$, where a monotonic convergence to the thermodynamic limit is recovered, the finite system is a reasonable representation of the infinite-length chain. For $S = 1$, at the smallest field we investigated, $h = 0.002$, we found $L_b \simeq 25$ (see lowest curve in the left panel of Fig. 1). This effect is more dramatic as S increases from 1 to 2. Fig. 1 clearly indicates that, for $S = 2$, and for the smallest applied field $h = 0.0001$, $L_b \simeq 70$, and that, even for $L \simeq 200$, the effect of the bump is not negligible, in the sense that the system appears to be far from an asymptotic convergence (see lowest curve in the right panel of Fig. 1). We shall address the physics underlying this behavior in Sec. III.

It should be clear that the presence of the bump strongly limits the possibility to draw reliable conclusions

from finite-size DMRG calculations, unless the latter are pushed to exceedingly large sizes, with huge numerical effort. On the other hand, only a careful extrapolation procedure can give insights on the actual thermodynamic limit. The infinite-size algorithm is certainly suitable for this kind of study.

Within our procedure we extract the thermodynamic limit for any given number of states N_k , by fitting the large- L behavior of the energy and magnetization as $e_0(h; L, N_k) = e_0^\infty(h; N_k) + A/L$ and $m(h; L, N_k) = m^\infty(h; N_k) + B/L$ respectively. The long-living corrections are $O(1/L)$ due to the OBC. We explicitly checked that the linear fit in $1/L$ at small field is accurate only if $L \gg L_b$. For the smallest field (and $S = 2$), we had to consider $L \simeq 1600$ to obtain a reliable result, and the situation gets worse at larger S [5].

Once $e_0^\infty(h; N_k)$ and $m^\infty(h; N_k)$ are obtained, we carefully check the convergence with respect to the Hilbert space, for both m and e_0 , by taking the extrapolation to the limit $N_k \rightarrow \infty$ in the region where the observables display a linear dependence on $1/N_k$ [6,7]. Up to $N_k = 150$ states were needed in the case $S = 2$ for the smallest field $h = 0.0001$, to obtain the linear scaling. We emphasize that this procedure explicitly deals with the convergence to the limit of infinite Hilbert space of the expectation values of the different observables, and is not equivalent to fixing a small truncation error *a priori*.

III. RESULTS AND DISCUSSION

In this section we mostly devote our analysis to the case $S = 2$, for which no results in the presence of the magnetic field can be found in the literature.

The groundstate energy per site e_0 extrapolated to the infinite-size limit ($L \rightarrow \infty$) and to the full Hilbert space ($N_k \rightarrow \infty$), is a smooth monotonically decreasing function of the magnetic field, correctly interpolating between the zero-field value $e_0(h = 0) = -4.76126(1)$, and the large-field asymptotic behavior $e_0(h \gg 1) \simeq -Sh$. The small-field region is plotted in Fig. 2, and the large-field region is shown in Fig. 3. Our result for $e_0(h = 0)$ is obtained by an extrapolation as a function of h , and the (relatively) large error bar is due to this procedure. The value compares reasonably well with Ref. [5] ($e_0 = -4.761244(1)$). Our value is slightly lower, suggesting that our extrapolation procedure is slightly more efficient than the one in Ref. [5].

The magnetization along the magnetic field can be either computed as outlined in Sec. II, by directly evaluating the expectation value of the corresponding operator \tilde{S}^z on the (approximate) DMRG groundstate wavefunction, or exploiting the Hellmann-Feynman theorem. The latter implies $\langle \tilde{S}_z \rangle = -\partial E_0 / \partial H$ when E_0 is an exact eigenvalue. m may therefore be estimated by a numerical derivative of the groundstate energy per site e_0 with

respect to the field amplitude h . It must be pointed out that when the wavefunction is not an exact eigenstate, as in the case of DMRG, the equality does not (necessarily) hold. However, if the state obtained within DMRG is close to an exact eigenstate, the Hellmann-Feynman relation is expected to hold within good accuracy.

The magnetization values obtained following the two procedures are shown in Fig. 4, and fall on a single regular curve. This remarkable agreement represents then a strong evidence of the convergence of our method with respect to the truncation of the Hilbert space, that may be used as a further check, besides the control of the truncation error \mathcal{R} , which is standard in DMRG [3], and the extrapolation to $N_k \rightarrow \infty$ explained in Sec. II.

The magnetization is a smooth function of h for all the values of the magnetic field, and correctly reproduces both the zero-field limit $m = 0$, and the $h \gg 1$ limit (shown in Fig. 5), where the curve saturates to 1. Nonetheless, a relatively sharp crossover at $h \simeq 0.005$ is signaled in Fig. 4 by a rapid change in the slope of the curve. The small- h region is characterized by a spin-liquid behavior, and the crossover can be naturally associated with a change in the nature of the ground-state from the spin-liquid state to a polarized Néel state, induced by a gradual freezing of quantum fluctuations. A further support of this interpretation comes from the analysis of the curves of m as a function of L shown in Fig. 1. The small- h region coincides indeed with the range in which the bump is observed in the curves. This finding sheds light on the physical origin of the bump. The bump can in fact be associated with a spin-liquid behavior, since it is observed only in this region.

If we now turn to the magnetization curves of Fig. 1, we can interpret the non-monotonicity in a simple way. When the system has a spin-liquid groundstate, it is characterized by a spin gap, and the correlation functions decay with a characteristic lengthscale ξ . If $L \ll \xi$, the system is too small to display the spin-liquid features, and behaves as if $\xi \rightarrow \infty$, i.e., similarly to a half-integer spin system, which responds more strongly to a small staggered external field. As a result, this leads to an “overshooting” of the magnetization, that assumes values larger than the thermodynamic limit. Only when $L \gg \xi$, the finite-system is representative of a spin liquid: the screening of the field becomes effective and the magnetization relaxes to its bulk value. This leads to an interpretation of L_b as an intrinsic lengthscale related to some correlation length ξ . A more quantitative study of this relationship requires a model for the evolution of the Haldane spin-liquid phase in the small-field region, and is currently underway [10].

A. The small-field region

As mentioned above, it is well known that the integer-spin AFM Heisenberg chain has a spin-liquid groundstate, characterized by a spin gap, the so-called Haldane gap. It is quite natural that the spin-liquid behavior extends to small finite fields. As a consequence, at the smallest field $h \simeq 0.0001$, the magnetization is linear in the field, as opposed to the half-integer spin case, which is critical (i.e. with divergent linear susceptibility) at zero field. Our (lower-bound) estimate of the linear susceptibility is $\chi(h = 0) = \frac{\partial m}{\partial h}|_{h=0} = 1070$, in extremely good agreement with the calculations in Ref. [2]. In this region the non-linear σ -model is therefore the most correct field theory. Unfortunately, the Haldane gap decreases by increasing the spin S , so that the field-driven crossover from the spin liquid to the antiferromagnet is expected to occur at an external field which decreases with increasing S ($h_c \sim 0.08$ for $S = 1$ and $h_c \sim 0.005$, for $S = 2$, as stated above). For $h > h_c$, the discrepancy with the non-linear σ -model results increases, even if a broad intermediate region exists, where the system is no longer a spin liquid, but the groundstate is not yet well described as a perturbation of the fully polarized antiferromagnet. In this intermediate region, the convergence of the magnetization to the thermodynamic limit is monotonic, and the asymptotic value is approached from below, contrary to the spin-liquid regime. Finally, a much smoother crossover takes place at larger fields, signaling the onset of a large-field “perturbative” region, where m monotonically approaches its limiting value from above, as we discuss in Sec. III B. We point out that the field-driven freezing of the quantum fluctuations is seen in the gradual simplification of the spectrum of the density matrix, i.e., a continuous reduction of the truncation error \mathcal{R} by increasing h at fixed N_k .

B. The large-field region

In the limit $h \rightarrow \infty$ the groundstate is trivially polarized. In this limit the spectrum of the density matrix is therefore dominated by a single state, with eigenvalue $w_1 = 1$, and the truncation error \mathcal{R} vanishes as soon as $N_k > 1$. It is therefore reasonable to expect that at large magnetic fields, $h \gg 1$, the spectrum of the density matrix will be much simpler than in the spin-liquid phase, making the convergence to the full Hilbert space relatively easy. As a consequence, the DMRG data are exceedingly accurate at $h = 1$, even by keeping $N_k \simeq 50$ states (giving $\mathcal{R} \sim 10^{-13}$), and at $h = 10$, keeping $N_k \simeq 30$ states (giving $\mathcal{R} \sim 10^{-16}$). Moreover, in this limit we can check our numerical data by comparison with the analytical results of standard perturbation theory around the $J = 0$ fully polarized groundstate.

The groundstate wavevector for the Hamiltonian (2) at $J = 0$ is $|0\rangle = |S\rangle_1 \dots |S\rangle_L$, with a groundstate energy $E_0^{(0)} = -HSL$. As the perturbation Hamiltonian is

$$\tilde{V} = -J \sum_{i=1}^{L-1} [\tilde{S}_i^z \tilde{S}_{i+1}^z + \frac{1}{2}(\tilde{S}_i^+ \tilde{S}_{i+1}^+ + \tilde{S}_i^- \tilde{S}_{i+1}^-)],$$

the groundstate energy up to second order in J is given by

$$E_0 \simeq E_0^{(0)} + \tilde{V}_{00} + \sum_{k>0} \frac{|\tilde{V}_{k0}|^2}{E_0^{(0)} - E_k^{(0)}}.$$

The excited states which contribute to the sum over k are all degenerate, and correspond to wavevectors of the form $|k\rangle = |S\rangle_1 \dots |S-1\rangle_k |S-1\rangle_{k+1} \dots |S\rangle_L$, $k = 1, \dots, L-1$, with unperturbed eigenvalues $E_k^{(0)} = -HSL + 2H$. As a result, for $h \gg 1$ we find

$$e_0 \simeq -hS \left[1 + S \frac{1}{h} + \frac{S}{2} \left(\frac{1}{h} \right)^2 \right] + \frac{S^2}{L} \left(1 + \frac{1}{2h} \right), \quad (3)$$

where the infinite-size value (first term in the r.h.s.) and the leading finite-size corrections $O(1/L)$ (second term in the r.h.s.), are explicitly shown. The agreement with the DMRG data for $h > 1$ is perfect, as shown in Fig. 3.

Analogously one can obtain the magnetization along the field, by calculating the groundstate wavefunction up to second order in perturbation theory, and then evaluating the expectation value of the operator \tilde{S}^z . It is however much simpler to make use of the Hellmann-Feynman theorem once more and calculate $\langle \tilde{S}^z \rangle = -\partial E_0 / \partial H \simeq SL - S^2(L-1)/(2h^2)$, obtaining

$$m \simeq \left(1 - \frac{S}{2h^2} \right) + \frac{S}{2h^2 L}. \quad (4)$$

We have thus found that the convergence to the thermodynamic limit [the first term in the r.h.s. of Eq. (4)] is monotonic and the finite-size corrections [the second term in the r.h.s. of Eq. (4)] are positive, in perfect agreement with the DMRG data (see Fig. 5). The deviation from the saturation value in the thermodynamic limit vanishes as $1/h^2$, in disagreement with the $1/\sqrt{h}$ behavior found within the nonlinear σ -model approach [2]. Since the calculation of Ref. [2] relies on the Haldane *ansatz*, the disagreement is expected at large magnetic fields, where the groundstate is Néel-like, rather than spin-liquid-like.

IV. CONCLUSIONS

We have presented extensive DMRG calculations for integer-spin antiferromagnetic Heisenberg chains in an external staggered magnetic field. The infinite-size DMRG algorithm has proven much more suitable than

the finite-size version, to extract the thermodynamic properties of these systems, due to the presence of sizeable characteristic lengthscales, which induce anomalous finite-size effects.

We have been able to determine three regions in the phase diagram of the $S = 2$ chain, as a function of the applied staggered field. The first region, for $0 < h \lesssim 0.005$ is the spin-liquid region, in which the spectrum is characterized by the Haldane gap, the spin susceptibility is linear in the field, with a coefficient $\chi(0) = 1070$, that compares extremely well with a non-linear σ -model calculation [2]. In this region the convergence of the magnetization to the thermodynamic limit is not monotonic as the system size L is increased, due to the existence of a characteristic lengthscale ξ . Thus, quite large systems must be considered to correctly describe the spin-liquid phase. Indeed, for $L \ll \xi$ the system is expected to behave as if $\xi \rightarrow \infty$, as it is the case for half-integer spin, with a strong increase of the magnetization. It is only for $L \gg \xi$ that the screening of the external field in the spin-liquid phase becomes effective and the magnetization can relax to its bulk value.

The second region ($0.005 \lesssim h \lesssim 1$) is an intermediate crossover region, where the system is no longer a spin liquid, due to the field-driven freezing of quantum fluctuations, but the field is not large enough to give rise to a linear antiferromagnet. As a result, both the non-linear σ -model (valid in the Haldane phase), and perturbation theory around the linear antiferromagnet (obviously valid for $h \rightarrow \infty$), are not accurate. In this region the magnetization curve monotonically approaches the thermodynamic limit, and the limit is reached from below (contrary to the Haldane phase).

Finally, for $h > 1$, the magnetic field is large enough to completely freeze quantum fluctuations and give rise to an almost saturated Néel antiferromagnet, that can be well described by perturbation theory in $1/h$. As predicted by perturbation theory, the magnetization decreases monotonically with increasing system size and approaches its thermodynamic limit from above.

A more detailed and quantitative comparison between our numerical results and the field-theoretical results of the nonlinear σ -model is presently in progress, aiming to clarify the identification of the characteristic length L_b observed in the DMRG data with some correlation length, and the precise region of validity of the analytical approaches [10].

ACKNOWLEDGMENTS

It is a pleasure to thank F. Becca for a substantial contribution to the improvement of the DMRG code. We also thank L. Capriotti, E. Ercolessi, G. Morandi, F. Ortolani, P. Pieri, M. Roncaglia, for stimulating discussions.

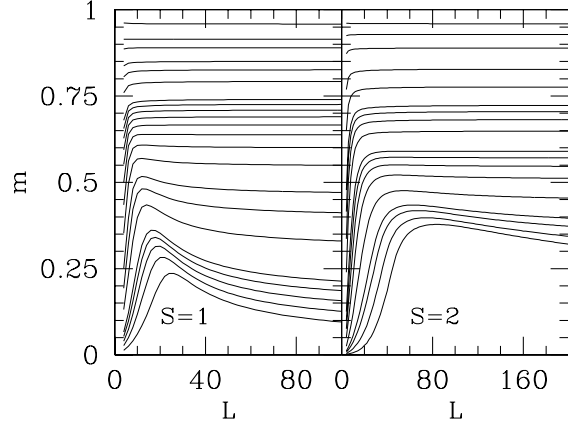


FIG. 1. Average magnetization m as a function of the length of the chain L , in the case $S = 1$ (left) and $S = 2$ (right), for $N_k = 50$. Notice the different scale on the L -axis. The different curves correspond to increasing values of the magnetic field, from bottom to top: in the left panel $h = 0.002, 0.004, 0.006, 0.008, 0.01, 0.02, 0.03, 0.04, 0.06, 0.08, 0.1, 0.12, 0.14, 0.16, 0.18, 0.2, 0.3, 0.4, 0.5, 0.75, 1.0, 2.0$; in the right panel $h = 0.0001, 0.0003, 0.0006, 0.0009, 0.002, 0.004, 0.006, 0.008, 0.01, 0.02, 0.03, 0.04, 0.05, 0.1, 0.2, 0.5, 1.0, 2.0$.

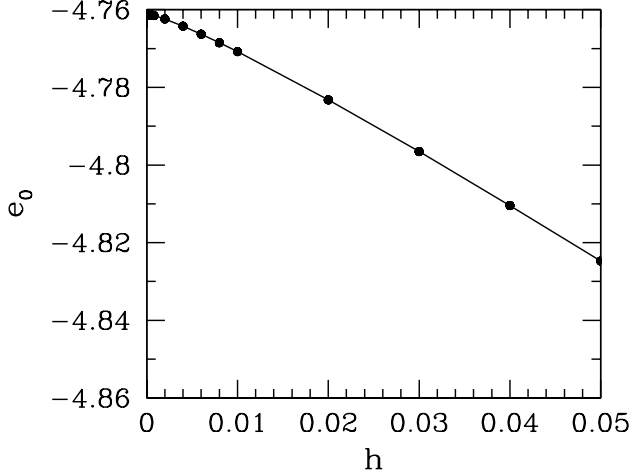


FIG. 2. Groundstate energy per site in the case $S = 2$, extrapolated to the thermodynamic limit $L \rightarrow \infty$ and to $N_k \rightarrow \infty$ (full circles), as a function of the magnetic field. The solid line is a guide to the eye.

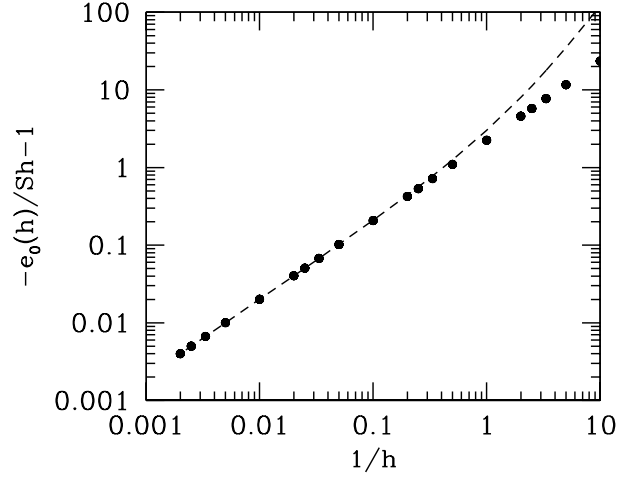


FIG. 3. Large-field behavior of the groundstate energy per site in the case $S = 2$ (full circles) compared with the second-order perturbation theory result, Eq. (3) for $L \rightarrow \infty$ (dashed line). To make the comparison more transparent $-e_0(h)/Sh - 1$ is plotted against $1/h$, in log-log scale.

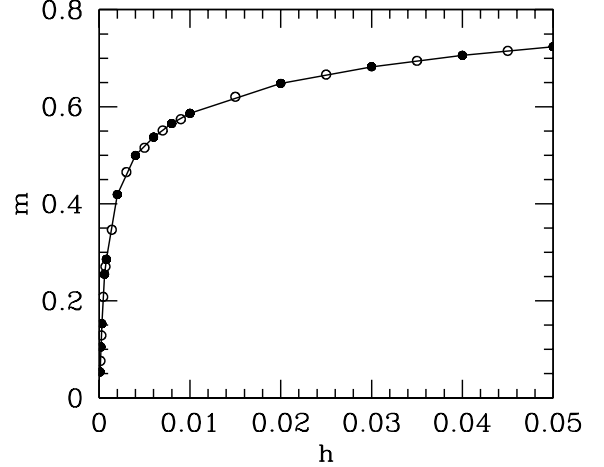


FIG. 4. Average magnetization per site m in the case $S = 2$, extrapolated to the thermodynamic limit $L \rightarrow \infty$ and to $N_k \rightarrow \infty$, as a function of the magnetic field. The full circles are direct DMRG measures, joined by the solid line as a guide to the eye, while the open dots are obtained by numerically differentiating the energy curve (see Fig. 2) according to the Hellmann-Feynman theorem.

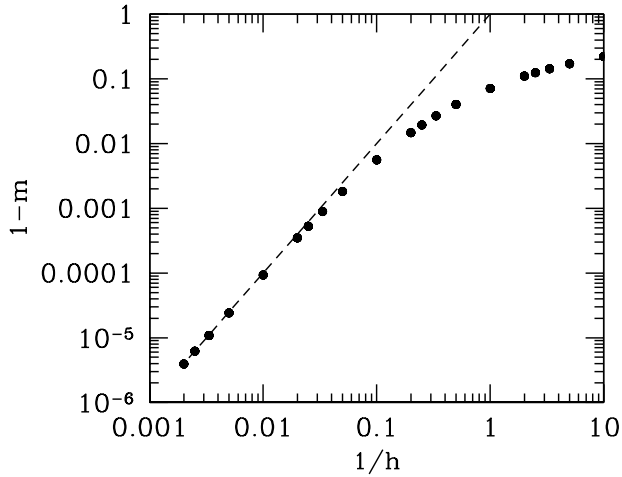


FIG. 5. Large-field behavior of the average magnetization per site m in the case $S = 2$ (full circles) compared with the perturbation theory result, Eq. (4) for $L \rightarrow \infty$ (dashed line). To make the comparison more transparent $1 - m$ is plotted against $1/h$, in log-log scale.

-
- [1] F. D. M. Haldane, Phys. Rev. Lett. **50**, 1153 (1983).
 - [2] E. Ercolessi, G. Morandi, P. Pieri, and M. Roncaglia, Europhys. Lett. **49**, 434 (2000); Phys. Rev. B **62**, 14 860 (2000); *e.print* cond-mat/0007188
 - [3] S. R. White, Phys. Rev. Lett. **69**, 2863 (1992); Phys. Rev. B **48**, 10 345 (1993).
 - [4] J. Lou, X. Dai, S. Qin, Z. Su, and Y. Lu, Phys. Rev. B **60**, 52 (1999).
 - [5] S. Qin, Y. Liu, Y. Lu, Phys. Rev. B **55**, 2721 (1997).
 - [6] A. Juozapavičius, S. Caprara, and A. Rosengren, Phys. Rev. B **56**, 11 097 (1997).
 - [7] A. Juozapavičius, L. Urba. S. Caprara, and A. Rosengren, Phys. Rev. B **60**, 14 771 (1999).
 - [8] see, e.g. the discussion in S. Caprara and A. Rosengren, Nucl. Phys. B **493**, 640 (1997); Europhys. Lett. **39**, 55 (1997). See also Refs. [6,7]
 - [9] S. Tsai and J. B. Marston, Phys. Rev. B **61**, 5546 (2000).
 - [10] M. Capone, S. Caprara, E. Ercolessi, G. Morandi, F. Ortolani, P. Pieri, and M. Roncaglia, in preparation.